It must however be borne in mind that the Jahn-Teller effects for the $5f^3$ ground state may well be much smaller than for the $5f^1$ Γ_8' level since not only are the ligand-field parameters reported[37] to be considerably smaller than for the earlier $[AnCl_6]^{2-}$ systems but in addition the Γ_8 ground level of $^4I_{9/2}$ should correlate most strongly with the strong-field states showing t_{2u} rather than t_{1u} orbital degeneracies, i.e., with the Γ_8 levels of $^2T_{2u}(a_{2u}^2t_{2u})$ and of $^2T_{1u}$ and $^4T_{1u}(a_{2u}t_{2u}^2)$. Nevertheless, further studies of the Np^{IV} hexahalo species and of the isoelectronic $CsPuF_6$ would obviously be of interest since the present work clearly indicates that f-orbital Jahn-Teller effects need not always be negligible.

(37) E. R. Menzel and J. R. Gruber, *J. Chem. Phys.*, **54**, 3857 (1971).

Registry No. $[CeF_6]^{3-}$, 72283-25-1; $[CeCl_6]^{3-}$, 27796-27-6; $[PaF_6]^{2-}$, 49864-66-6; $[PaCl_6]^{2-}$, 44463-14-1; $[PaBr_6]^{2-}$, 44463-09-4; $[PaI_6]^{2-}$, 44463-23-2; $[UF_6]^-$, 48021-45-0; $[UCl_6]^-$, 44491-58-9; $[UBr_6]^-$, 44491-06-7.

Contribution from the Department of Chemistry, University of California, Los Angeles, California 90024

Spin-State Isomerism of Tris(2-picolylamine)iron(II). The Diiodide and the Hydrated Dichloride

BRADLEY A. KATZ and CHARLES E. STROUSE*

Received June 5, 1979

Crystal structure determinations of tris(2-picolylamine)iron(II) dichloride dihydrate and tris(2-picolylamine)iron(II) diiodide have accounted for the anomalous magnetic susceptibility of the diiodide and have demonstrated that both the *fac* and *mer* isomers of this complex can exhibit spin-equilibrium behavior. The influence of the complex geometry on the thermodynamics of the spin transformation is discussed. In the dichloride dihydrate lattice the tris(2-picolylamine)iron(II) cation, $Fe(2\text{-pic})_3^{2+}$, adopts the *fac* configuration with approximate threefold symmetry and an average iron-nitrogen bond length at 115 K of 1.997 (2) Å indicative of the low-spin state. A three-dimensional hydrogen-bonding network links the noncoordinating chloride ions, the water molecules, and all six amine hydrogens of the complex. At 115 K the dichloride conforms to space group $P\bar{1}$ with $Z = 2$, $a = 10.099$ (4) Å, $b = 10.541$ (3) Å, $c = 11.272$ (4) Å, $\alpha = 114.11$ (3)°, $\beta = 98.77$ (3)°, $\gamma = 94.05$ (3)°, $V = 1071$ (1) Å^3, $R = 0.030$, and $R_w = 0.042$ for 4377 observed reflections. Two crystallographically independent isomers of the $Fe(2\text{-pic})_3^{2+}$ complex are found in the diiodide lattice. The unsymmetrical *mer* isomer, with an average iron-nitrogen bond length of 2.200 (7) Å, is high spin, while the *fac* isomer, with an average bond length of 2.064 (6) Å, exists as an interconverting mixture of high-spin and low-spin species at room temperature. The *mer* and *fac* isomers are linked together through hydrogen-bonding interactions between the iodide ions and the amine hydrogen atoms of both isomers. At room temperature the diiodide conforms to space group $P\bar{1}$ with $Z = 4$, $a = 11.649$ (3) Å, $b = 16.933$ (6) Å, $c = 16.271$ (5) Å, $\alpha = 116.86$ (2)°, $\beta = 92.92$ (2)°, $\gamma = 120.02$ (2)°, $V = 2314$ (1) Å^3, $R = 0.038$ and $R_w = 0.045$ for 4362 observed reflections.

Introduction

Observation of spin isomerism in certain transition-metal complexes has prompted a number of efforts to appraise those factors that influence the energetics of spin-state transformations. Changes in nonmagnetic and noncoordinating counterions and molecules of solvation have been found to produce pronounced changes in the magnetic properties of both iron(II) and iron(III) complexes. Among the complexes that have been investigated are $[Fe^{II}paptH_2]X_2$,[1,2] $Fe^{II}(pyim)_3(ClO_4)_2$,[3] $[Fe^{II}(pyben)_3]X_2$,[4] $[Fe^{III}(sal)_2trien]X$,[5] $Fe^{III}(S_2CNC_4H_8O)_3$,[6] and $Fe^{II}(2\text{-pic})_3Cl_2\cdot S$[7-9] where S = $2H_2O$, MeOH, and EtOH. The energy differences responsible for these magnetic changes are relatively small (a few kcal), and as a result, such factors as hydrogen bonding, geometric isomerism, and van der Waals interactions can all play significant roles.

The study reported herein is the second in a series of investigations of the solid-state spin transformations of the $Fe^{II}(2\text{-pic})_3^{2+}$(2-pic = 2-picolylamine) dication. Multiple-temperature structural investigations of the *mer* isomer of this ion, described in the initial report,[9] demonstrated the feasibility of crystallographic resolution of spin isomers and elucidated the structural relationships between the ethanol and methanol solvates of tris(2-picolylamine)iron(II) dichloride. In the present investigation structural observations pertinent to the spin dynamics of the *fac* isomer are reported and related to those previously provided.

Experimental Section

Preparation of Compounds. $Fe(2\text{-pic})_3I_2$. To a 0.1 M aqueous solution of $FeCl_2\cdot 4H_2O$ was added, under N_2, 3 equiv of 2-picolylamine (Aldrich Chemicals, 99%) whereupon a dark red solution formed. A 20-fold excess of KI dissolved in a minimum volume of deoxygenated (N_2) water was added to this solution. Dark red diamond-shaped crystals of $Fe(2\text{-pic})_3I_2$ formed when the resulting solution was cooled in an ice-salt water bath.

$Fe(2\text{-pic})_3Cl_2\cdot 2H_2O$. To a concentrated aqueous solution of $FeCl_2\cdot 4H_2O$ was added, under N_2, 3 equiv of 2-picolylamine. The dark red solution was evaporated under nitrogen. Red crystals of the dihydrate formed after approximately 1 week.

Data Collection. $Fe(2\text{-pic})_3I_2$. A tetrahedrally shaped crystal of volume 0.0064 mm^3 was attached to a glass fiber and mounted on a Syntex $P\bar{1}$ diffractometer. Automatic centering of 15 strong reflections with graphite-monochromatized Mo Kα radiation (λ 0.710 70

(1) Sylva, R. N.; Goodwin, H. A. *Aust. J. Chem.* **1967**, *20*, 479.
(2) Sylva, R. N.; Goodwin, H. A. *Aust. J. Chem.* **1968**, *21*, 1081.
(3) Goodgame, D. M. L.; Machado, A. A. S. C. *Chem. Commun.* **1969**, 1420.
(4) Sams, J. R.; Tsin, T. B. *Inorg. Chem.* **1976**, *15*, 1544.
(5) Sinn, E.; Sim, G.; Dose, E. V.; Tweedle; M. F.; Wilson, L. J. *J. Am. Chem. Soc.* **1978**, *100*, 3375.
(6) Butcher, R. J.; Sinn, E. *J. Am. Chem. Soc.* **1976**, *98*, 5159.
(7) Sorai, M.; Ensling, J.; Hasselbach, K. M.; Gütlich, P. *Chem. Phys.* **1977**, *20*, 197.
(8) Greenaway, A. M.; Sinn, E. *J. Am. Chem. Soc.* **1978**, *100*, 8080.
(9) Katz, B. A.; Strouse, C. E. *J. Am. Chem. Soc.* **1979**, *101*, 6214.

0020-1669/80/1319-0658$01.00/0

Å) yielded triclinic lattice parameters: a = 11.649 (3) Å, b = 16.933 (6) Å, c = 16.271 (5) Å, α = 116.86 (2)°, β = 92.92 (2)°, γ = 120.02 (2)°, V = 2314 (1) Å^3. The experimental density of 1.84 g/cm^3 measured by the flotation method (carbon tetrachloride–bromoethane) agreed with the calculated density of 1.820 g/cm^3 based on four formula units of $Fe(2\text{-pic})_3I_2$ per unit cell.

Previously described data handling procedures were employed in this work.[10] A hemisphere of intensity data for which $2\theta < 45°$ was collected at 2.0°/min in the θ–2θ scan mode from 1.2° below $K\alpha_1$ to 1.0° above $K\alpha_2$. The total background time was equal to the total peak scan time. The calculated transmission coefficients (based on a linear absorption coefficient of 34.0 cm^{-1} for Mo $K\alpha$ radiation) fell within the range of 0.46–0.67 and were applied to the data during the course of the refinement. A total of 4362 reflections for which $I > 3\sigma(I)$ were used in the solution and final refinement of the structure.

$Fe(2\text{-pic})_3Cl_2\cdot 2H_2O$. A crystal of approximate dimensions 0.30 × 0.15 × 0.10 mm was attached to a glass fiber (long axis parallel to the fiber axis) and transferred into the nitrogen stream of a locally constructed variable-temperature apparatus[11] mounted on a Syntex $P\bar{1}$ diffractometer. Temperature control, measurements, and stability of the device have been described previously.[9] A least-squares fit of 15 strong reflections automatically centered at 115 K with Mo $K\alpha$ radiation yielded triclinic lattice parameters: a = 10.099 (4) Å, b = 10.541 (3) Å, c = 11.272 (4) Å, α = 114.11 (3)°, β = 98.77 (3)°, γ = 94.05 (3)°, V = 1070.7 (6) Å^3. The density determined at room temperature by the flotation method (carbon tetrachloride–pentane) was 1.49 g/cm^3 whereas the calculated density at 115 K based on two formula units of $Fe(2\text{-pic})_3Cl_2\cdot 2H_2O$ per unit cell was 1.573 g/cm^3.

Intensity data were collected in the θ–2θ scan mode from 1.7° below the $K\alpha_1$ peak to 1.5° above the $K\alpha_2$ peak at a scan rate of 4.0°/min. The total background count time was equal to the total peak scan time. A first data set for which $2\theta(\text{max}) = 50°$ and a second shell of data for which $50° < 2\theta < 60°$ and $h < 6$ were collected. The combined data sets provided 4377 observed reflections ($I > 3\sigma(I)$). Because of the small and regular cross section of this crystal, no absorption correction was applied.

Solution and Refinement of the Structures. $Fe(2\text{-pic})_3I_2$. A three-dimensional Patterson map[12] yielded the positions of the four pairs of centrosymmetrically related iodide ions and of the two crystallographically independent iron(II) ions, consistent with assignment of $P\bar{1}$ as the space group. All the nonhydrogen atomic positions were obtained from the first Fourier synthesis.

Full-matrix least-squares refinement of positional and anisotropic thermal parameters of all nonhydrogen atoms was carried out. Scattering factors were taken from ref 13. Anomalous dispersion corrections for iron and iodine were used in all structure factor calculations. After initial refinement to R = 0.042 and R_w = 0.050, estimated positions for the hydrogen atoms were calculated (C–H and N–H = 1.00 Å) and fixed. These atoms were assigned isotropic thermal parameters of 4.5 Å^2 and included in subsequent structure factor calculations. After convergence of the refinement at R = 0.038 and R_w = 0.045, a difference Fourier map revealed no peaks larger than one of intensity 1.1 e/Å^3 in the vicinity of I(4). The final standard deviation of an observation of unit weight was 1.45.

Table I gives atomic positional and thermal parameters with estimated standard deviations for the nonhydrogen atoms as determined in the final least-squares cycle. A listing of observed structure factor amplitudes from the data obtained and calculated structure factor amplitudes based on the parameters of the final least-squares refinement is available as supplementary material.

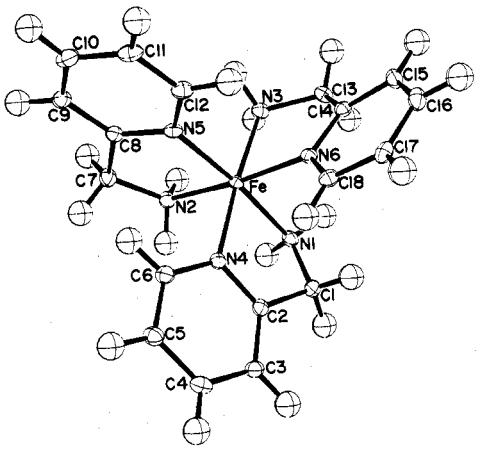

Figure 1. ORTEP diagram[12] of the *fac* complex ion in $Fe(2\text{-pic})_3Cl_2\cdot 2H_2O$ at 115 K viewed down the approximate threefold axis of the complex. For clarity the hydrogen atoms in this and other diagrams have not been labeled.

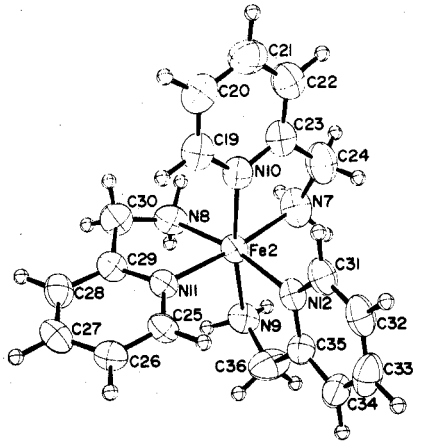

Figure 2. ORTEP diagram of the *fac* isomer of $Fe(2\text{-pic})_3I_2$ viewed down the threefold axis of the complex. The thermal ellipsoids of hydrogen atoms were reduced for clarity.

$Fe(2\text{-pic})_3Cl_2\cdot 2H_2O$. Standard Patterson, Fourier, and least-squares techniques were employed to solve the structure at 115 K. Anomalous dispersion corrections for iron and for chlorine were used in all structure factor calculations. After initial refinement to R = 0.069 and R_w = 0.111, the positions of all nonwater hydrogen atoms were calculated (C–H and N–H = 1.00 Å) and included in subsequent structure factor calculations with isotropic thermal parameters of 1.40 Å^2. A difference Fourier map yielded the positions of the water hydrogens; isotropic thermal parameters of these hydrogen atoms were fixed at a value found for the oxygen atoms to which they are bound (1.20 Å^2). The refinement of the positional and anisotropic thermal parameters of all nonhydrogen atoms converged at R = 0.030 and R_w = 0.042 with a standard deviation in observation of unit weight of 1.47. A final difference Fourier map revealed no peaks larger than 0.4 e/Å^3. Table II provides atomic positional and thermal parameters with estimated standard deviations from the final least-squares cycle. A listing of observed and calculated structure factor amplitudes is available as supplementary material.[14]

Results and Discussion

$Fe(2\text{-pic})_3Cl_2\cdot 2H_2O$. The three bidentate 2-picolylamine ligands form a distorted octahedron around the Fe(II) ion. A pseudo-threefold axis of the *fac*-$Fe(2\text{-pic})_3^{2+}$ ion passes through

(10) Strouse, J.; Layten, S. W.; Strouse, C. E. *J. Am. Chem. Soc.* **1977**, *99*, 562.

(11) Strouse, C. E. *Rev. Sci. Instrum.* **1976**, *47*, 871.

(12) The programs used in this work included data reduction programs written at UCLA: JBPATT, JBFOUR, and PEAKLIST, modified versions of Fourier programs written by J. Blount; UCLA versions of ORFLS (Busing, Martin, and Levy), structure factor calculations and full matrix, least-squares refinement; ORTEP (Johnson), figure plotting; ABSN (Coppens), absorption correction; and ORFFE (Busing, Martin, and Levy), distance, angle, and error computations. The equations used in data reduction are the same as given in: Wilkerson, A. K.; Chodak, J. B.; Strouse, C. E. *J. Am. Chem. Soc.* **1975**, *97*, 3000. All least-squares refinements computed the agreement factors R and R_w according to $R = \sum||F_o| - |F_c||/\sum|F_o|$ and $R_w = [\sum w_i||F_o| - |F_c||^2/\sum w_i|F_o|^2]^{1/2}$, where F_o and F_c are the observed and calculated structure factors, respectively, and $w_i^{1/2} = 1/\sigma(F_o)$. The parameter minimized in all least-squares refinements was $\sum w_i||F_o| - |F_c||^2$. All calculations were performed on the IBM 360-91KK computer operated by the UCLA Campus Computing Network.

(13) "International Tables for X-ray Crystallography"; Kynoch Press: Birmingham, England, 1974; Vol. IV.

(14) Complete structural information for $Fe(2\text{-pic})_3Cl_2\cdot 2H_2O$ at room temperature is also available in the supplementary material.

Table I. Atomic Positions and Temperature Factors ($\times 10^4$) for $Fe(2\text{-pic})_3I_2$ [a]

atom	x	y	z	B_{11} [c]	B_{22}	B_{33}	B_{12}	B_{13}	B_{23}
I(1)	0.2844 (1)	0.8375 (1)	0.2149 (1)	141 (1)	88 (1)	126 (1)	69 (1)	38 (1)	61 (1)
I(2)	0.1879 (1)	0.1237 (0)	0.4724 (0)	79 (1)	80 (1)	81 (0)	35 (1)	22 (0)	34 (0)
I(3)	-0.0190 (1)	0.0699 (0)	0.1559 (0)	144 (1)	77 (1)	75 (0)	49 (1)	46 (1)	50 (0)
I(4)	0.0908 (1)	0.4836 (1)	0.3291 (1)	80 (1)	140 (1)	116 (1)	42 (1)	34 (1)	94 (1)
Fe(1)	0.4167 (1)	0.7553 (1)	0.6602 (1)	73 (1)	56 (1)	73 (1)	33 (1)	28 (1)	38 (1)
Fe(2)	0.1702 (1)	0.2303 (1)	0.8168 (1)	77 (1)	44 (1)	47 (1)	24 (1)	13 (1)	25 (1)
N(1)	0.2172 (7)	0.5930 (6)	0.5920 (5)	84 (9)	71 (6)	88 (6)	36 (6)	24 (6)	48 (5)
N(2)	0.4492 (7)	0.7506 (5)	0.5258 (5)	93 (9)	73 (6)	81 (5)	50 (6)	35 (6)	42 (5)
N(3)	0.6306 (7)	0.9075 (5)	0.7493 (6)	104 (9)	63 (6)	87 (6)	44 (6)	38 (6)	42 (5)
N(4)	0.4832 (7)	0.6486 (5)	0.6403 (4)	102 (9)	53 (5)	54 (4)	43 (6)	25 (5)	29 (4)
N(5)	0.2980 (7)	0.8102 (5)	0.6240 (5)	103 (9)	79 (6)	73 (5)	58 (6)	43 (6)	45 (5)
N(6)	0.4270 (7)	0.8111 (5)	0.8142 (5)	76 (9)	53 (5)	77 (5)	28 (6)	19 (6)	32 (5)
C(1)	0.6170 (9)	0.6783 (7)	0.6542 (6)	126 (13)	82 (8)	59 (6)	73 (9)	35 (7)	37 (6)
C(2)	0.6545 (11)	0.6110 (9)	0.6443 (6)	193 (16)	101 (10)	57 (6)	103 (11)	44 (8)	41 (7)
C(3)	0.5509 (14)	0.5054 (9)	0.6153 (7)	260 (21)	127 (12)	62 (7)	147 (14)	55 (10)	53 (8)
C(4)	0.4112 (12)	0.4725 (7)	0.5997 (6)	275 (21)	63 (7)	57 (6)	95 (11)	47 (9)	38 (6)
C(5)	0.3804 (9)	0.5455 (7)	0.6127 (6)	154 (14)	60 (7)	48 (6)	48 (9)	21 (7)	31 (5)
C(6)	0.2331 (10)	0.5153 (7)	0.6000 (8)	112 (13)	66 (8)	104 (8)	23 (8)	36 (8)	42 (7)
C(7)	0.1914 (10)	0.8079 (7)	0.6526 (6)	141 (13)	87 (8)	68 (6)	73 (9)	44 (8)	38 (6)
C(8)	0.1068 (9)	0.8259 (8)	0.6141 (7)	120 (13)	96 (9)	67 (7)	79 (9)	16 (8)	22 (7)
C(9)	0.1350 (11)	0.8512 (8)	0.5461 (7)	172 (16)	93 (9)	56 (7)	97 (10)	6 (8)	15 (6)
C(10)	0.2455 (10)	0.8566 (7)	0.5159 (6)	170 (14)	75 (8)	48 (6)	78 (9)	23 (7)	20 (5)
C(11)	0.3247 (8)	0.8336 (6)	0.5560 (6)	107 (11)	55 (7)	55 (6)	45 (7)	20 (7)	23 (5)
C(12)	0.4424 (9)	0.8348 (7)	0.5247 (7)	124 (12)	72 (8)	87 (7)	56 (8)	47 (8)	50 (6)
C(13)	0.3185 (9)	0.7688 (7)	0.8439 (7)	113 (13)	74 (8)	85 (8)	45 (8)	44 (8)	47 (7)
C(14)	0.3360 (11)	0.8024 (8)	0.9402 (8)	164 (16)	96 (9)	99 (9)	73 (11)	67 (10)	65 (8)
C(15)	0.4712 (13)	0.8839 (9)	1.0125 (7)	213 (19)	98 (10)	70 (7)	98 (12)	38 (10)	44 (7)
C(16)	0.5811 (10)	0.9270 (7)	0.9823 (7)	132 (14)	69 (8)	68 (7)	56 (9)	3 (8)	23 (6)
C(17)	0.5573 (9)	0.8915 (7)	0.8845 (7)	100 (12)	69 (7)	79 (7)	53 (8)	33 (8)	41 (6)
C(18)	0.6782 (9)	0.9399 (7)	0.8521 (8)	83 (11)	68 (8)	102 (8)	30 (8)	26 (8)	42 (7)
N(7)	0.0386 (8)	0.1894 (6)	0.6924 (5)	151 (11)	61 (6)	54 (5)	30 (7)	9 (6)	26 (5)
N(8)	0.0070 (6)	0.1504 (5)	0.8587 (5)	74 (8)	65 (6)	80 (6)	29 (6)	20 (6)	41 (5)
N(9)	0.1689 (7)	0.0927 (5)	0.7371 (5)	106 (9)	43 (5)	66 (5)	28 (6)	22 (5)	29 (4)
N(10)	0.1662 (6)	0.3649 (5)	0.8759 (5)	76 (8)	70 (6)	50 (5)	31 (6)	12 (5)	31 (5)
N(11)	0.2860 (6)	0.2736 (5)	0.9485 (4)	74 (8)	48 (5)	55 (4)	27 (5)	20 (5)	33 (4)
N(12)	0.3456 (6)	0.2945 (5)	0.7818 (4)	99 (8)	46 (5)	39 (4)	28 (6)	11 (5)	22 (4)
C(19)	0.2118 (8)	0.4420 (7)	0.9720 (6)	90 (11)	65 (7)	57 (6)	25 (8)	19 (7)	31 (6)
C(20)	0.1935 (10)	0.5240 (7)	1.0062 (7)	135 (14)	73 (8)	65 (7)	44 (9)	36 (8)	31 (6)
C(21)	0.1271 (11)	0.5290 (8)	0.9372 (9)	155 (15)	102 (10)	110 (9)	83 (10)	73 (10)	69 (9)
C(22)	0.0810 (9)	0.4514 (8)	0.8390 (7)	129 (13)	88 (9)	75 (7)	54 (9)	31 (8)	50 (7)
C(23)	0.1033 (9)	0.3709 (7)	0.8111 (6)	105 (11)	68 (7)	56 (6)	33 (8)	16 (7)	33 (6)
C(24)	0.0592 (10)	0.2875 (9)	0.7064 (7)	176 (16)	114 (10)	58 (7)	69 (11)	18 (8)	47 (7)
C(25)	0.4264 (8)	0.3194 (6)	0.9812 (6)	76 (10)	57 (6)	60 (6)	32 (7)	16 (6)	37 (5)
C(26)	0.4912 (8)	0.3342 (6)	1.0642 (6)	102 (11)	58 (7)	56 (6)	45 (7)	17 (7)	26 (5)
C(27)	0.4132 (9)	0.3029 (7)	1.1187 (6)	129 (13)	65 (7)	56 (6)	49 (8)	7 (7)	32 (6)
C(28)	0.2697 (9)	0.2567 (7)	1.0866 (6)	139 (13)	66 (7)	63 (6)	51 (8)	38 (7)	44 (6)
C(29)	0.2101 (8)	0.2437 (6)	1.0022 (6)	81 (10)	47 (6)	60 (6)	24 (6)	19 (6)	33 (5)
C(30)	0.0549 (8)	0.1981 (7)	0.9647 (7)	86 (11)	89 (8)	82 (7)	42 (8)	35 (7)	55 (7)
C(31)	0.4249 (9)	0.3961 (6)	0.8002 (6)	116 (12)	57 (7)	53 (5)	31 (8)	14 (7)	34 (5)
C(32)	0.5516 (10)	0.4376 (7)	0.7845 (7)	145 (14)	74 (8)	72 (7)	43 (9)	34 (8)	55 (6)
C(33)	0.5985 (9)	0.3735 (9)	0.7472 (7)	106 (12)	109 (10)	64 (7)	37 (10)	34 (7)	53 (7)
C(34)	0.5178 (9)	0.2685 (7)	0.7264 (6)	140 (13)	85 (8)	58 (6)	66 (9)	49 (7)	44 (6)
C(35)	0.3916 (8)	0.2322 (6)	0.7437 (6)	116 (11)	54 (6)	47 (5)	45 (7)	28 (6)	27 (5)
C(36)	0.3040 (10)	0.1221 (7)	0.7269 (8)	167 (15)	62 (7)	121 (9)	69 (9)	73 (10)	51 (7)

atom [b]	x	y	z	atom [b]	x	y	z
C(22)H	0.0324	0.4579	0.7893	N(2)H(3)	0.3732	0.6758	0.4639
N(8)H(3)	−0.0349	0.0692	0.8201	C(12)H(1)	0.5372	0.9091	0.5714
N(8)H(2)	−0.0749	0.1539	0.8389	C(12)H(2)	0.4299	0.8215	0.4565
N(9)H(3)	0.0902	0.0412	0.6693	C(6)H(1)	0.2060	0.5133	0.6570
N(9)H(2)	0.1415	0.0519	0.7711	C(6)H(2)	0.1617	0.4395	0.5377
N(7)H(3)	−0.0650	0.1335	0.6777	C(7)H	0.1685	0.7892	0.7060
N(7)H(2)	0.0598	0.1527	0.6311	C(8)H	0.0203	0.8169	0.6305
C(3)OH(2)	−0.0046	0.1392	0.9784	C(9)H	0.0758	0.8683	0.5192
C(3)OH(1)	0.0403	0.2565	0.9998	C(10)H	0.2647	0.8765	0.4627
C(36)H(2)	0.2863	0.0637	0.6573	C(13)H	0.2165	0.7078	0.7920
C(36)H(1)	0.3556	0.1163	0.7742	C(14)H	0.2534	0.7702	0.9627
C(24)H(2)	−0.0349	0.2649	0.6644	C(15)H	0.4874	0.9096	1.0853
C(28)H	0.2120	0.2358	1.1275	C(16)H	0.6835	0.9886	1.0356
C(27)H	0.4588	0.3113	1.1797	C(1)H	0.6951	0.7555	0.6733
C(26)H	0.5986	0.3688	1.0882	C(2)H	0.7572	0.6346	0.6577
C(25)H	0.4876	0.3449	0.9434	C(3)H	0.5664	0.4490	0.6018
C(34)H	0.5545	0.2219	0.6983	C(4)H	0.3323	0.3927	0.5798
C(33)H	0.6955	0.4077	0.7365	C(18)H(1)	0.7396	0.9137	0.8537
C(32)H	0.6109	0.5143	0.7991	C(18)H(2)	0.7429	1.0225	0.8943
C(31)H	0.3931	0.4461	0.8280	N(3)H(2)	0.6978	0.8991	0.7158
C(19)H	0.2634	0.4426	1.0247	N(3)H(3)	0.6303	0.9678	0.7494

Table I (*Continued*)

atom[b]	x	y	z	atom[b]	x	y	z
C(20)H	0.2290	0.5804	1.0810	N(1)H(2)	0.1467	0.6007	0.6232
C(21)H	0.1118	0.5879	0.9580	N(1)H(3)	0.1742	0.5642	0.5192
C(24)H(1)	0.1313	0.3172	0.6765	N(2)H(2)	0.5441	0.7632	0.5239

[a] At room temperature. [b] For all atoms in this section, $B = 4.50$ Å^2. [c] Temperature factors of the form $\exp(-(B_{11}h^2 + B_{22}k^2 + B_{33}l^2 + 2B_{12}hk + 2B_{13}hl + 2B_{23}kl))$.

Table II. Atomic Positions and Temperature Factors ($\times 10^4$) for $Fe(2\text{-pic})_3Cl_2 \cdot 2H_2O$[a]

atom	x	y	z	B_{11}[b]	B_{22}	B_{33}	B_{12}	B_{13}	B_{23}
Cl(1)	0.9335 (1)	0.8906 (0)	0.2383 (0)	42 (1)	42 (0)	28 (0)	6 (0)	6 (0)	13 (0)
Cl(2)	0.2097 (0)	0.5867 (0)	0.9175 (0)	29 (1)	40 (0)	31 (0)	5 (0)	8 (0)	20 (0)
Fe	0.2647 (0)	0.3690 (0)	0.1726 (0)	23 (0)	25 (0)	19 (0)	3 (0)	3 (0)	12 (0)
N(1)	0.1271 (2)	0.4836 (2)	0.1337 (2)	25 (2)	38 (2)	32 (1)	4 (1)	5 (1)	21 (1)
N(2)	0.3205 (2)	0.3187 (2)	−0.0040 (2)	29 (2)	38 (2)	27 (1)	7 (1)	7 (1)	19 (1)
N(3)	0.1303 (2)	0.1903 (2)	0.0984 (1)	34 (2)	33 (2)	24 (1)	3 (1)	4 (1)	13 (1)
N(4)	0.3825 (2)	0.5524 (2)	0.2446 (1)	26 (2)	31 (1)	23 (1)	6 (1)	6 (1)	16 (1)
N(5)	0.4114 (2)	0.2651 (2)	0.2020 (1)	30 (2)	23 (1)	25 (1)	0 (1)	0 (1)	10 (1)
N(6)	0.2016 (2)	0.3978 (2)	0.3378 (1)	25 (2)	27 (1)	25 (1)	4 (1)	3 (1)	14 (1)
C(1)	0.1653 (2)	0.6306 (2)	0.2364 (2)	29 (2)	35 (2)	36 (2)	9 (2)	9 (2)	19 (1)
C(2)	0.3166 (2)	0.6652 (2)	0.2673 (2)	30 (2)	35 (2)	23 (1)	8 (2)	9 (1)	16 (1)
C(3)	0.3849 (2)	0.8015 (2)	0.3177 (2)	45 (2)	28 (2)	32 (2)	7 (2)	13 (2)	14 (1)
C(4)	0.5252 (2)	0.8231 (2)	0.3452 (2)	43 (2)	33 (2)	31 (2)	−3 (2)	4 (2)	16 (1)
C(5)	0.5938 (2)	0.7078 (2)	0.3179 (2)	30 (2)	38 (2)	40 (2)	1 (2)	2 (2)	20 (1)
C(6)	0.5192 (2)	0.5755 (2)	0.2678 (2)	28 (2)	34 (2)	34 (2)	4 (2)	2 (1)	17 (1)
C(7)	0.4477 (2)	0.2574 (2)	−0.0090 (2)	35 (2)	48 (2)	33 (2)	14 (2)	13 (2)	23 (1)
C(8)	0.4851 (2)	0.2190 (2)	0.1053 (2)	30 (2)	27 (2)	28 (2)	2 (1)	6 (1)	12 (1)
C(9)	0.5930 (2)	0.1454 (2)	0.1132 (2)	31 (2)	32 (2)	46 (2)	4 (2)	6 (2)	17 (1)
C(10)	0.6293 (2)	0.1204 (2)	0.2244 (2)	36 (2)	32 (2)	51 (2)	5 (2)	−2 (2)	20 (2)
C(11)	0.5542 (2)	0.1668 (2)	0.3234 (2)	44 (2)	33 (2)	37 (2)	4 (2)	−5 (2)	19 (1)
C(12)	0.4462 (2)	0.2359 (2)	0.3086 (2)	43 (2)	32 (2)	27 (2)	3 (2)	2 (1)	13 (1)
C(13)	0.0305 (2)	0.2052 (2)	0.1855 (2)	31 (2)	34 (2)	30 (2)	−4 (2)	3 (1)	16 (1)
C(14)	0.0964 (2)	0.3035 (2)	0.3255 (2)	26 (2)	30 (2)	30 (2)	7 (1)	4 (1)	17 (1)
C(15)	0.0499 (2)	0.3012 (2)	0.4348 (2)	28 (2)	47 (2)	40 (2)	9 (2)	13 (2)	26 (2)
C(16)	0.1081 (2)	0.4031 (2)	0.5605 (2)	37 (2)	59 (2)	32 (2)	19 (2)	13 (2)	26 (2)
C(17)	0.2111 (2)	0.5051 (2)	0.5731 (2)	35 (2)	43 (2)	24 (2)	19 (2)	5 (1)	14 (1)
C(18)	0.2565 (2)	0.4973 (2)	0.4614 (2)	33 (2)	30 (2)	27 (2)	7 (2)	1 (1)	13 (1)
O(1)	0.1900 (2)	0.9132 (1)	0.1081 (2)	58 (2)	47 (1)	53 (1)	16 (1)	22 (1)	28 (1)
O(2)	0.1732 (2)	0.9374 (2)	0.4984 (2)	51 (2)	107 (2)	42 (1)	28 (2)	14 (1)	15 (1)

atom	x	y	z	B, Å^2	atom	x	y	z	B, Å^2
C(12)H	0.3903	0.2612	0.3808	1.40	C(7)H(1)	0.4374	0.1701	−0.0969	1.40
C(15)H	−0.0265	0.2262	0.4244	1.40	C(7)H(2)	0.5232	0.3266	−0.0090	1.40
C(16)H	0.0716	0.4047	0.6409	1.40	C(1)H(1)	0.1240	0.6989	0.2016	1.40
C(17)H	0.2499	0.5799	0.6634	1.40	C(1)H(2)	0.1281	0.6446	0.3181	1.40
C(18)H	0.3324	0.5724	0.4765	1.40	N(3)H(1)	0.0840	0.1638	0.0057	1.40
C(11)H	0.5808	0.1505	0.4036	1.40	N(2)H(2)	0.3299	0.4055	−0.0181	1.40
C(10)H	0.7049	0.0648	0.2334	1.40	N(2)H(1)	0.2445	0.2487	−0.0739	1.40
C(9)H	0.6526	0.1131	0.0445	1.40	N(1)H(2)	0.0342	0.4431	0.1338	1.40
C(6)H	0.5710	0.4919	0.2432	1.40	N(1)H(1)	0.1272	0.4792	0.0423	1.40
C(5)H	0.6954	0.7203	0.3340	1.40	N(3)H(3)	0.1798	0.1068	0.0976	1.40
C(4)H	0.5759	0.9203	0.3869	1.40	O(2)H(1)	0.0972	0.9306	0.4306	1.20
C(3)H	0.3335	0.8862	0.3352	1.40	O(2)H(2)	0.1422	0.9972	0.5763	1.20
C(13)H(1)	−0.0484	0.2479	0.1543	1.40	O(1)H(1)	0.1960	0.8194	0.0609	1.20
C(13)H(2)	−0.0100	0.1118	0.1789	1.40	O(1)H(2)	0.1248	0.9028	0.1506	1.20

[a] At 115 K. [b] Temperature factors of the form $\exp(-(B_{11}h^2 + B_{22}k^2 + B_{33}l^2 + 2B_{12}hk + 2B_{13}hl + 2B_{23}kl))$.

the midpoint of the face comprising the pyridine nitrogens and through that comprising the amine nitrogens (see Figure 1). These two faces are rotated by $\theta = 5.6°$ from octahedral toward trigonal prismatic geometry. Similar distortions have been observed in other chelate complexes.[15,16] The average iron–nitrogen bond length of 1.997 (2) Å is consistent with the low-spin state. The three Fe–N(amine) bond lengths are slightly greater than the three Fe–N(pyridine) bond lengths with averages of 2.020 (1) Å vs. 1.974 (1) Å at 115 K. These lengths are slightly shorter than those observed in low-spin *mer*-$Fe(2\text{-pic})_3Cl_2 \cdot MeOH$ (Fe–N(amine) = 2.033 (3) Å vs. Fe–N(pyridine) = 2.000 (3) Å). The ligand bite angles of ca. 82° are also typical of the low-spin state. Iron–nitrogen bond lengths and bond angles are summarized in Table III. Tables IV and V give bond lengths and bond angles, respectively, within the 2-picolylamine ligands.

$Fe(2\text{-pic})_3I_2$. The crystallographically independent unit of this salt consists of a *fac*-$Fe(2\text{-pic})_3^{2+}$ ion, a *mer*-$Fe(2\text{-pic})_3^{2+}$ ion, and four noncoordinated iodide ions.[17] In the *fac* complex ion, all iron–nitrogen bond lengths (Table III) are significantly longer (Fe–N(av) = 2.063 (6) Å at room temperature) than

(15) Hoselton, M. A.; Wilson, L. J.; Drago, R. S. *J. Am. Chem. Soc.* **1975**, *97*, 1722.
(16) Mealli, C.; Lingafelter, E. C. *Chem. Commun.* **1970**, 885.

(17) König, E.; Ritter, G.; Madeja, K.; Böhmer, W. A. *J. Phys. Chem. Solids* **1972**, *33*, 327. $Fe_3(bpy)_7(NCS)_6$ and $Fe_3(bpy)_7(NCSe)_6$ contain low-spin and high-spin iron(II) in a 2:1 ratio within the same lattice, independent of temperature. From infrared spectra, it was concluded that NCS and NCSe groups are in the cis arrangement for the low-spin complex and that from restrictions in the space group the high-spin unit is trans.

Table III. Iron–Nitrogen Bond Distances and Angles in $Fe(2\text{-pic})_3Cl_2\cdot 2H_2O$ and in $Fe(2\text{-pic})_3I_2$[a]

	$Fe(2\text{-pic})_3Cl_2\cdot 2H_2O$[b]		$Fe(2\text{-pic})_3I_2$[c] cis isomer		$Fe(2\text{-pic})_3I_2$[c] trans isomer	
			Distances, Å			
amine	Fe–N(1)	2.016 (2)	Fe(2)–N(7)	2.069 (7)	Fe(1)–N(3)[d]	2.187 (7)
amine	Fe–N(2)	2.020 (2)	Fe(2)–N(9)	2.085 (6)	Fe(1)–N(2)	2.212 (7)
amine	Fe–N(3)	2.025 (2)	Fe(2)–N(8)	2.074 (6)	Fe(1)–N(1)[d]	2.185 (7)
	Fe–N(amine)		Fe–N(amine)	2.076 (6)	Fe–N(amine)	2.195 (7)
pyridine	Fe–N(4)	1.977 (2)	Fe(2)–N(10)	2.061 (7)	Fe(1)–N(6)	2.214 (7)
pyridine	Fe–N(5)	1.970 (2)	Fe(2)–N(12)	2.033 (6)	Fe(1)–N(5)[d]	2.196 (7)
pyridine	Fe–N(6)	1.974 (2)	Fe(2)–N(11)	2.060 (6)	Fe(1)–N(4)[d]	2.206 (6)
	Fe–N(pyridine)	1.974 (2)	Fe–N(pyridine)	2.051 (6)	Fe–N(pyridine)	2.205 (7)
	Fe–N(av)	1.997 (2)	Fe–N(av)	2.063 (6)	Fe–N(av)	2.200 (7)
			Angles, Deg			
ligand bite angle	N(1)–Fe–N(4)	81.19 (7)	N(7)–Fe(2)–N(10)	80.1 (3)	N(1)–Fe(1)–N(4)	75.8 (2)
ligand bite angle	N(2)–Fe–N(5)	83.38 (7)	N(8)–Fe(2)–N(11)	79.7 (2)	N(2)–Fe(1)–N(5)	75.5 (2)
ligand bite angle	N(3)–Fe–N(6)	82.50 (7)	N(9)–Fe(2)–N(12)	80.0 (2)	N(3)–Fe(1)–N(6)	76.0 (3)
	N(1)–Fe–N(2)	92.13 (7)	N(7)–Fe(2)–N(8)	95.2 (3)	N(2)–Fe(1)–N(3)	89.7 (3)
	N(2)–Fe–N(3)	91.82 (7)	N(8)–Fe(2)–N(9)	91.7 (3)	N(3)–Fe(1)–N(4)	94.7 (2)
	N(1)–Fe–N(3)	93.98 (7)	N(7)–Fe(2)–N(9)	92.2 (3)	N(2)–Fe(1)–N(4)	92.2 (2)
	N(4)–Fe–N(5)	94.99 (7)	N(10)–Fe(2)–N(11)	95.9 (2)	N(5)–Fe(1)–N(6)	99.3 (2)
	N(5)–Fe–N(6)	94.94 (7)	N(11)–Fe(2)–N(12)	92.7 (2)	N(1)–Fe(1)–N(5)	89.1 (3)
	N(4)–Fe–N(6)	96.29 (7)	N(10)–Fe(2)–N(12)	96.3 (2)	N(1)–Fe(1)–N(6)	96.0 (3)
	N(2)–Fe–N(4)	89.51 (7)	N(7)–Fe(2)–N(12)	92.8 (3)	N(1)–Fe(1)–N(2)	99.5 (3)
	N(3)–Fe–N(5)	89.91 (7)	N(8)–Fe(2)–N(10)	93.0 (3)	N(3)–Fe(1)–N(5)	102.3 (3)
	N(1)–Fe–N(6)	89.90 (7)	N(9)–Fe(2)–N(11)	92.0 (2)	N(4)–Fe(1)–N(6)	97.0 (2)
	N(1)–Fe–N(5)	174.15 (6)	N(7)–Fe(2)–N(11)	173.5 (3)	N(1)–Fe(1)–N(3)	166.9 (3)
	N(2)–Fe–N(6)	174.09 (6)	N(8)–Fe(2)–N(12)	168.6 (3)	N(2)–Fe(1)–N(6)	163.5 (2)
	N(3)–Fe–N(4)	175.04 (7)	N(9)–Fe(2)–N(10)	171.4 (3)	N(4)–Fe(1)–N(5)	158.6 (2)
	Fe–N(1)–C(1)	108.0 (1)	Fe(2)–N(7)–C(24)	109.6 (5)	Fe(1)–N(3)–C(18)	113.0 (5)
	Fe–N(2)–C(7)	111.9 (1)	Fe(2)–N(9)–C(36)	111.3 (5)	Fe(1)–N(2)–C(12)	108.3 (5)
	Fe–N(3)–C(13)	109.8 (1)	Fe(2)–N(8)–C(30)	111.7 (5)	Fe(1)–N(1)–C(6)	113.6 (5)
	Fe–N(4)–C(2)	115.3 (1)	Fe(2)–N(10)–C(23)	115.3 (6)	Fe(1)–N(6)–C(17)	116.0 (5)
	Fe–N(5)–C(8)	115.9 (1)	Fe(2)–N(12)–C(35)	116.2 (5)	Fe(1)–N(5)–C(11)	114.6 (5)
	Fe–N(6)–C(14)	115.7 (1)	Fe(2)–N(11)–C(29)	115.8 (5)	Fe(1)–N(4)–C(5)	116.7 (5)
	Fe–N(4)–C(6)	127.1 (1)	Fe(2)–N(10)–C(19)	127.3 (6)	Fe(1)–N(6)–C(13)	126.8 (6)
	Fe–N(5)–C(12)	126.8 (1)	Fe(2)–N(12)–C(31)	126.2 (5)	Fe(1)–N(5)–C(7)	126.4 (6)
	Fe–N(6)–C(18)	126.8 (1)	Fe(2)–N(11)–C(25)	126.3 (5)	Fe(1)–N(4)–C(1)	125.3 (5)

[a] Uncertainties in bond length averages are the averages of the individual esd's. [b] At 115 K. [c] At room temperature. [d] Trans.

Table IV. Bond Distances (Å) within the 2-Picolylamine Ligands in $Fe(2\text{-pic})_3Cl_2\cdot 2H_2O$ and in $Fe(2\text{-pic})_3I_2$

$Fe(2\text{-pic})_3Cl_2\cdot 2H_2O$[a]		$Fe(2\text{-pic})_3I_2$[b] *fac* isomer		$Fe(2\text{-pic})_3I_2$[b] *mer* isomer	
N(1)–C(1)	1.484 (3)	N(7)–C(24)	1.457 (12)	N(1)–C(6)	1.476 (12)
N(2)–C(7)	1.477 (3)	N(8)–C(30)	1.459 (10)	N(2)–C(12)	1.475 (10)
N(3)–C(13)	1.484 (3)	N(9)–C(36)	1.438 (11)	N(3)–C(18)	1.476 (11)
N(4)–C(2)	1.355 (2)	N(10)–C(19)	1.345 (10)	N(4)–C(1)	1.345 (9)
N(4)–C(6)	1.351 (3)	N(10)–C(23)	1.324 (10)	N(4)–C(5)	1.352 (10)
N(5)–C(8)	1.358 (3)	N(11)–C(25)	1.353 (9)	N(5)–C(7)	1.337 (10)
N(5)–C(12)	1.361 (2)	N(11)–C(29)	1.354 (9)	N(5)–C(11)	1.336 (10)
N(6)–C(14)	1.353 (2)	N(12)–C(31)	1.349 (9)	N(6)–C(13)	1.347 (10)
N(6)–C(18)	1.355 (2)	N(12)–C(35)	1.339 (9)	N(6)–C(17)	1.348 (10)
C(1)–C(2)	1.498 (3)	C(23)–C(24)	1.475 (12)	C(5)–C(6)	1.496 (12)
C(7)–C(8)	1.505 (3)	C(29)–C(30)	1.517 (11)	C(11)–C(12)	1.481 (11)
C(13)–C(14)	1.501 (3)	C(35)–C(36)	1.484 (11)	C(17)–C(18)	1.498 (12)
C(2)–C(3)	1.392 (3)	C(19)–C(20)	1.376 (12)	C(1)–C(2)	1.362 (11)
C(3)–C(4)	1.385 (3)	C(20)–C(21)	1.387 (13)	C(2)–C(3)	1.377 (14)
C(4)–C(5)	1.389 (3)	C(21)–C(22)	1.370 (13)	C(3)–C(4)	1.395 (14)
C(5)–C(6)	1.383 (3)	C(22)–C(23)	1.392 (12)	C(4)–C(5)	1.385 (12)
C(8)–C(9)	1.394 (3)	C(25)–C(26)	1.362 (10)	C(7)–C(8)	1.367 (12)
C(9)–C(10)	1.385 (3)	C(26)–C(27)	1.384 (11)	C(8)–C(9)	1.356 (13)
C(10)–C(11)	1.387 (3)	C(27)–C(28)	1.383 (11)	C(9)–C(10)	1.377 (12)
C(11)–C(12)	1.380 (3)	C(28)–C(29)	1.375 (11)	C(10)–C(11)	1.389 (11)
C(14)–C(15)	1.392 (3)	C(31)–C(32)	1.378 (12)	C(13)–C(14)	1.365 (12)
C(15)–C(16)	1.386 (3)	C(32)–C(33)	1.370 (13)	C(14)–C(15)	1.393 (13)
C(16)–C(17)	1.390 (3)	C(33)–C(34)	1.384 (12)	C(15)–C(16)	1.367 (13)
C(17)–C(18)	1.378 (3)	C(34)–C(35)	1.383 (11)	C(16)–C(17)	1.375 (12)

[a] At 115 K. [b] At room temperature.

Table V. Bond Angles (Deg) within the 2-Picolylamine Ligands and Water Molecules of $Fe(2\text{-pic})_3Cl_2\cdot 2H_2O$ and of $Fe(2\text{-pic})_3I_2$

$Fe(2\text{-pic})_3Cl_2\cdot 2H_2O$[a]		$Fe(2\text{-pic})_3I_2$[b] *fac* isomer		$Fe(2\text{-pic})_3I_2$[b] *mer* isomer	
N(1)-C(1)-C(2)	108.3 (2)	N(7)-C(24)-C(23)	112.2 (7)	N(1)-C(6)-C(5)	112.1 (7)
N(2)-C(7)-C(8)	111.3 (2)	N(8)-C(30)-C(29)	109.5 (7)	N(2)-C(12)-C(11)	109.3 (7)
N(3)-C(13)-C(14)	109.2 (2)	N(9)-C(36)-C(35)	113.0 (7)	N(3)-C(18)-C(17)	112.9 (7)
C(1)-C(2)-C(3)	123.3 (2)	C(24)-C(23)-C(22)	121.4 (9)	C(6)-C(5)-C(4)	121.7 (9)
C(7)-C(8)-C(9)	121.5 (2)	C(30)-C(29)-C(28)	122.1 (7)	C(12)-C(11)-C(10)	120.9 (8)
C(13)-C(14)-C(15)	122.5 (2)	C(36)-C(35)-C(34)	120.4 (7)	C(18)-C(17)-C(16)	120.5 (8)
C(2)-C(3)-C(4)	119.0 (2)	C(23)-C(22)-C(21)	119.3 (9)	C(5)-C(4)-C(3)	119.7 (9)
C(8)-C(9)-C(10)	119.5 (2)	C(29)-C(28)-C(27)	119.0 (7)	C(11)-C(10)-C(9)	118.1 (8)
C(14)-C(15)-C(16)	119.3 (2)	C(35)-C(34)-C(33)	118.1 (8)	C(17)-C(16)-C(15)	120.9 (8)
C(3)-C(4)-C(5)	119.2 (2)	C(22)-C(21)-C(20)	118.8 (9)	C(4)-C(3)-C(2)	118.2 (8)
C(9)-C(10)-C(11)	118.5 (2)	C(28)-C(27)-C(26)	118.4 (7)	C(10)-C(9)-C(8)	120.1 (8)
C(15)-C(16)-C(17)	118.6 (2)	C(34)-C(33)-C(32)	119.2 (8)	C(16)-C(15)-C(14)	117.0 (9)
C(4)-C(5)-C(6)	118.5 (2)	C(21)-C(20)-C(19)	118.0 (9)	C(3)-C(2)-C(1)	119.2 (9)
C(10)-C(11)-C(12)	119.5 (2)	C(27)-C(26)-C(25)	120.0 (7)	C(9)-C(8)-C(7)	118.8 (8)
C(16)-C(17)-C(18)	119.0 (2)	C(33)-C(32)-C(31)	119.4 (8)	C(15)-C(14)-C(13)	119.8 (9)
C(5)-C(6)-N(4)	123.3 (2)	C(20)-C(19)-N(10)	120.6 (9)	C(2)-C(1)-N(4)	123.5 (8)
C(11)-C(12)-N(5)	122.9 (2)	C(26)-C(25)-N(11)	122.3 (7)	C(8)-C(7)-N(5)	123.1 (8)
C(17)-C(18)-N(6)	123.2 (2)	C(32)-C(31)-N(12)	122.4 (8)	C(14)-C(13)-N(6)	123.1 (8)
C(6)-N(4)-C(2)	117.6 (2)	C(19)-N(10)-C(23)	117.2 (7)	C(1)-N(4)-C(5)	118.0 (7)
C(12)-N(5)-C(8)	117.2 (2)	C(25)-N(11)-C(29)	117.6 (6)	C(7)-N(5)-C(11)	118.2 (7)
C(18)-N(6)-C(14)	117.5 (2)	C(31)-N(12)-C(35)	117.4 (7)	C(13)-N(6)-C(17)	117.1 (8)
N(4)-C(2)-C(1)	114.4 (2)	N(10)-C(23)-C(24)	115.8 (8)	N(4)-C(5)-C(6)	117.0 (7)
N(5)-C(8)-C(7)	116.1 (2)	N(11)-C(29)-C(30)	115.2 (7)	N(5)-C(11)-C(12)	117.4 (7)
N(6)-C(14)-C(13)	115.1 (2)	N(12)-C(35)-C(36)	116.1 (7)	N(6)-C(17)-C(18)	117.3 (8)
N(4)-C(2)-C(3)	122.3 (2)	N(10)-C(23)-C(22)	122.7 (8)	N(4)-C(5)-C(4)	121.3 (9)
N(5)-C(8)-C(9)	122.3 (2)	N(11)-C(29)-C(28)	122.7 (7)	N(5)-C(11)-C(10)	121.7 (8)
N(6)-C(14)-C(15)	122.3 (2)	N(12)-C(35)-C(34)	123.4 (7)	N(6)-C(17)-C(16)	122.1 (8)
O(1)H(2)-O(1)-O(1)H(1)[c]	98.4 (1)				
O(2)H(2)-O(2)-O(2)H(1)[c]	99.5 (2)				

[a] At 115 K. [b] At room temperature. [c] Water molecules.

those in the dihydrate (Fe–N(av) = 1.997 (2) Å at 115 K or 2.006 (2) Å at room temperature[8]). The *fac* isomer of $Fe(2\text{-pic})_3I_2$ is depicted in Figure 2. From the increase in the average iron–nitrogen bond distances toward the high-spin values of 2.200 (7) Å observed for the *mer* isomer in the same material, it is estimated that about 30% of *fac*-$Fe(2\text{-pic})_3I_2$ exists in the high-spin state. The twist angle, $\theta = 10°$, is greater than that in the low-spin dihydrate, in keeping with the previously noted trend[18] in some spin equilibrium tris(dithiocarbamato)iron(III) complexes that as the equilibrium is shifted to favor the high-spin state, the resulting increase in iron–ligand bond lengths is associated with an increase in θ. The average ligand bite angle of ca. 80° (Table III) is also significantly less than that for the low-spin dihydrate (82°), as expected if some high-spin *fac*-$Fe(2\text{-pic})_3I_2$ is present. The occurrence of a spin transition in the *fac* isomer near room temperature is also consistent with the gradual increase in the effective magnetic moment near room temperature.[19] Because of the large thermal motion at room temperature, no attempt was made to crystallographically resolve the spin isomers in *fac*-$Fe(2\text{-pic})_3I_2$. Bond distances and bond angles within the 2-picolylamine ligands of the *fac* isomer are presented in Tables IV and V.

The *mer* isomer of $Fe(2\text{-pic})_3I_2$ is shown in Figure 3. Iron–nitrogen bond distances and bond angles appear in Table III; Tables IV and V provide bond distances and angles within the ligands. The average iron–nitrogen bond length of 2.200 (7) Å compares well with values of 2.198 (6) and 2.188 (3) Å for the predominantly high-spin methanol and ethanol solvates of *mer*-$Fe(2\text{-pic})_3Cl_2$, respectively.[9] The average ligand bite angle of 76° is substantially less than that for the low-spin dihydrate (82°), for the low-spin–high-spin *fac* isomer of the diiodide (80°) (Table III), and for low-spin methanol solvate (82°)[9] but similar to that in the high-spin methanol (76°) and ethanol solvates (76°).

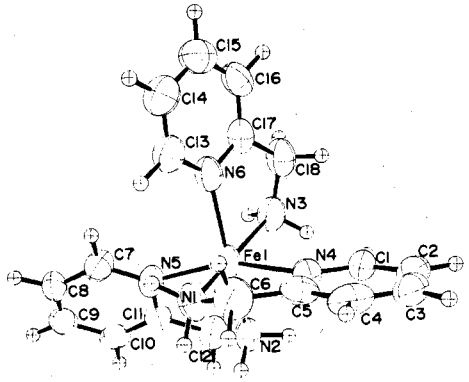

Figure 3. ORTEP diagram of the *mer* isomer of $Fe(2\text{-pic})_3I_2$.

π Bonding. As in the high-spin methanol and ethanol solvates of *mer*-$Fe(2\text{-pic})_3Cl_2$, the Fe–N(amine) and Fe–N(pyridine) distances of the *mer* complex in $Fe(2\text{-pic})_3I_2$ are nearly equivalent (2.195 (7) Å vs. 2.205 (7) Å). However, this is not the case for the low-spin *fac* dihydrate (2.020 (2) Å vs. 1.974 (2) Å), the predominantly low-spin *fac* diiodide (2.076 (6) Å vs. 2.051 (6) Å), or the low-spin *mer* methanol solvate (2.033 (3) Å vs. 2.000 (3) Å). The shorter Fe–N(pyridine) bond distances for both *fac* and *mer* low-spin $Fe(2\text{-pic})_3^{2+}$ complexes can be rationalized as resulting from significant interactions between the T_{2g} (in O_h) orbitals on the low-spin iron(II) ion with pyridine π orbitals. If the complex undergoes a transition to the high-spin state, such interactions decrease, as two electrons are promoted from the π-bonding

(18) Healy, P. C.; White, A. H. *J. Chem. Soc., Dalton Trans.* **1972**, 1163.
(19) Renovitch, G. A.; Baker, W. A. *J. Am. Chem. Soc.* **1967**, *89*, 6377.

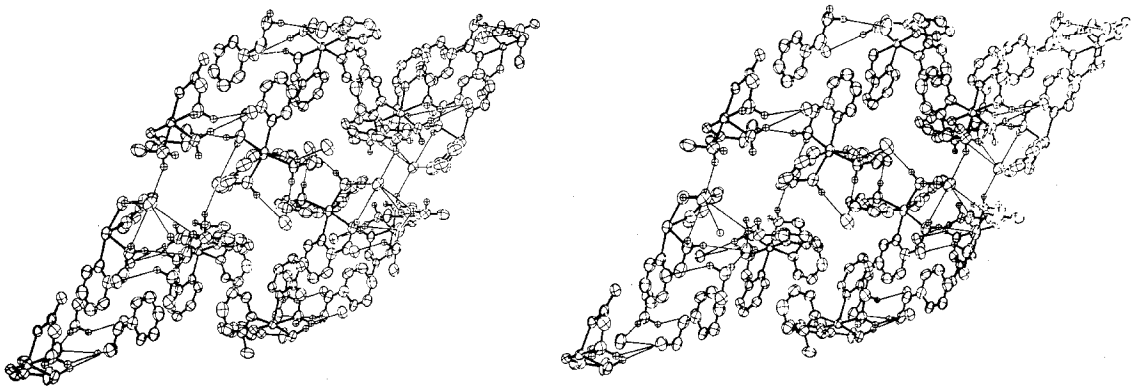

Figure 4. Stereoscopic ORTEP pair of the $Fe(2\text{-pic})_3I_2$ lattice showing the hydrogen-bonding network. The phenyl and methylene hydrogens have been omitted for clarity. The view is down the *a* axis with the *c** axis in the vertical direction.

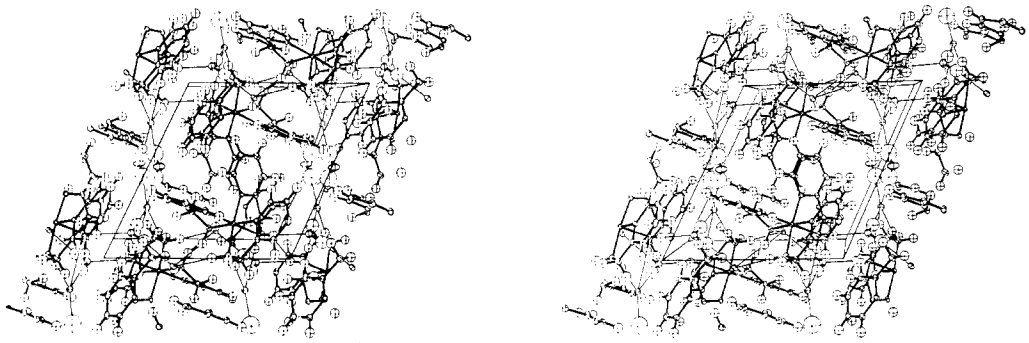

Figure 5. Stereoscopic ORTEP pair of the $Fe(2\text{-pic})_3Cl_2 \cdot 2H_2O$ lattice showing the hydrogen-bonding network. The view is down the *a* axis with the *c** axis in the vertical direction.

Table VI. Hydrogen-Bonding Interactions (Å) in $Fe(2\text{-pic})_3Cl_2 \cdot 2H_2O$ and in $Fe(2\text{-pic})_3I_2$[a]

$Fe(2\text{-pic})_3Cl_2 \cdot 2H_2O$[b]		$Fe(2\text{-pic})_3I_2$[c]			
		cis isomer		trans isomer	
N(1)H(1)-Cl(2)[d]	2.341	N(7)H(1)-I(2)	3.021	N(1)H(1)-I(4)[e]	2.749
N(1)H(2)-Cl(2)[e]	2.410	N(7)H(2)-I(1)[e]	3.280	N(1)H(2)-I(4)	2.637
N(2)H(1)-Cl(1)[f]	2.238	N(7)H(2)-I(2)[j]	3.282	N(2)H(1)-I(2)[k]	2.703
N(2)H(2)-Cl(2)[d]	2.614	N(9)H(1)-I(3)[j]	2.671	N(2)H(2)-I(4)	2.885
N(3)H(1)-Cl(1)[f]	2.544	N(9)H(2)-I(2)[j]	2.824	N(3)H(1)-I(2)[k]	3.340
N(3)H(2)-O(1)[g]	2.101	N(8)H(1)-I(1)[e]	2.645	N(3)H(2)-I(1)[i]	2.669
O(1)H(1)-Cl(2)[d]	2.351	N(8)H(2)-I(3)[j]	2.894		
O(1)H(2)-Cl(1)[h]	2.319				
O(2)H(1)-Cl(1)[h]	2.382				
O(2)H(2)-Cl(1)[i]	2.225				

[a] Hydrogen atomic positions were not refined. [b] At 115 K. [c] At room temperature. [d] $x, y, z-1$. [e] $-x, 1-y, 1-z$. [f] $1-x, 1-y, -z$. [g] $x, y-1, z$. [h] $x-1, y, z$. [i] $1-x, 2-y, 1-z$. [j] $-x, -y, 1-z$. [k] $1-x, 1-y, 1-z$.

T_{2g} orbitals to the antibonding E_g orbitals. The result is longer and more nearly equivalent Fe–N bond lengths.

This argument can also be used to rationalize the observation that in $Fe(2\text{-pic})_3I_2$ the *fac* isomer is predominantly low spin and the *mer* isomer completely high spin at room temperature. While the symmetry of the *fac* isomer is correct for the overlap of the three ligand LUMO's with the three T_{2g} orbitals, the *mer* isomer allows overlap of these three ligand LUMO's with only two T_{2g} orbitals. This is also reflected in the shorter average iron–nitrogen bond length for the low-spin *fac* isomer (1.997 (2) Å for the dihydrate at 115 K) than for the low-spin *mer* isomer (2.016 (3) Å for the methanol solvate at 115 K).

Hydrogen Bonding. In the diiodide lattice, the four iodide ions are hydrogen bonded to the amine hydrogen atoms of the complex ions, linking alternately *fac* and *mer* isomers in a complex network (Figure 4). The observed NH–I bond lengths are listed in Table VI. In view of the fact that the closest approach to an iodide, I(1), of a nonamine hydrogen atom, C(34)H, is 3.071 Å, the interactions N(7)H(2)–I(1) = 3.800, N(7)H(2)–I(2) = 3.282, and N(3)H(1)–I(2) = 3.340 Å probably do not produce significant hydrogen bonding, but they are included for completeness.

In a multiple temperature crystallographic investigation of the methanol and ethanol solvates of $Fe(2\text{-pic})_3Cl_2$,[9] both structures were observed to have the same two-dimensional hydrogen-bonding network linking the noncoordinating chloride ions to all six amine hydrogen atoms and to the alcohol molecules. The dihydrate exhibits a three-dimensional hydrogen-bonding network, linking the chloride ions, the water molecules, and the six amine hydrogen atoms (Figure 5); the hydrogen bond lengths are presented in Table VI. One water molecule, water 2, joins through its hydrogen atoms two chloride ions, Cl(2), related by a center of symmetry. Chloride ion Cl(1) is also bound to two amine hydrogens, N(2)H(1) and N(3)H(1), from two ligands of a complex ion and to a hydrogen atom of the second water molecule, water 1. The other hydrogen atom of water 1 is bound to the second chlo-

ride, Cl(2). The oxygen atom of water 1 is bound to an amine hydrogen atom N(3)H(2) of a complex ion related to the first by a center of symmetry. The second chloride, Cl(2), is bound to an amine hydrogen atom, N(1)H(2), of the complex and to two amine hydrogen atoms, N(1)H(1) and N(2)H(2), of two ligands of another centrosymmetrically related complex. Thus five of the amine hydrogen atoms of a single complex are bound to chloride ions, while the sixth is bound to the oxygen atom of a water of crystallization.

Hydrogen bonding between amine donor atoms and water has also been observed in $[Fe^{III}(sal)_2trien]Cl\cdot 2H_2O$ and $[Fe^{III}(sal)_2trien]NO_3\cdot H_2O$,[5] both of which exhibit chain hydrogen-bonding networks. The fact that both compounds are low spin at room temperature has been attributed to the strong NH–O hydrogen-bonding interactions favoring the low-spin state. Greenaway and Sinn,[8] in their room-temperature investigations of low-spin *fac*-$Fe(2\text{-pic})_3Cl_2\cdot 2H_2O$ and high-spin *mer*-$Fe(2\text{-pic})_3Cl_2\cdot CH_3OH$, suggest that the difference in room-temperature spin states can be attributed to the presence of a NH–O interaction in the former but not in the latter. (In both these compounds all amine hydrogen atoms not involved in hydrogen bonding to oxygen atoms do exhibit interactions with the chloride ions.) While the *fac* complex in the dihydrate, which is low spin both at 115 K and at room temperature, exhibits an NH–O interaction, the *fac* isomer of the diiodide, which is predominantly low spin at room temperature, has no such interaction. The *mer* isomer of the diiodide and the *mer* complexes in the methanol and ethanol solvates of the dichloride all lack NH–O interactions and are all high spin at room temperature. These results suggest that the room-temperature spin state in tris(2-picolylamine)iron(II) complexes is influenced more strongly by the complex geometry than by the hydrogen bonding. The comparison of iron–amine and iron–pyridine bond distances presented above supports the hypothesis that the *fac* geometry stabilizes the low-spin electronic configuration.

Acknowledgment. This work was supported by the UCLA research committee, the UCLA office of Academic Computing, and the National Science Foundation (Grant CHE78-01564). Bradley A. Katz was supported by a UCLA chancellor's fellowship and Charles E. Strouse acknowledges the support of an Alfred P. Sloan research fellowship.

Registry No. *fac*-$Fe(2\text{-pic})_3I_2$, 72228-92-3; *mer*-$Fe(2\text{-pic})_3I_2$, 72244-68-9; *fac*-$Fe(2\text{-pic})_3Cl_2\cdot 2H_2O$, 68889-84-9.

Supplementary Material Available: A listing of atomic positional and thermal parameters at room temperature for the dihydrate, a table of bond distances and angles at room temperature for the dihydrate, a table of hydrogen-bonding interactions for the dihydrate, and a listing of observed and calculated structure factors for the dihydrate at 115 K and at room temperature and for the diiodide at room temperature (44 pages). Ordering information is given on any current masthead page.

Contribution from the Laboratoire de Chimie de Coordination du CNRS, Associé à l'Université Paul Sabatier, 31400 Toulouse, France

Synthesis and Crystal and Molecular Structure of the 2:1 Molecular Adduct between *N,N'*-(1,2-Phenylene)bis(salicylaldiminato)copper(II) and 7,7,8,8-Tetracyanoquinodimethane

PATRICK CASSOUX* and ALAIN GLEIZES*

Received July 11, 1979

A molecular adduct (2:1) between a tetradentate Schiff base complex, *N,N'*-(1,2-phenylene)bis(salicylaldiminato)copper(II) [Cu(salphen)], and 7,7,8,8-tetracyanoquinodimethane (TCNQ) is described. The conditions necessary to obtain this adduct are very critical, and the solution electronic spectra of the mixed component molecules show a new band at ~4300 Å, with respect to the spectra of the starting materials, only several hours after mixing. This adduct crystallizes in the triclinic system, space group $P\bar{1}$, with cell constants a = 11.970 (4) Å, b = 12.567 (4) Å, c = 7.020 (2) Å, α = 103.44 (2)°, β = 92.35 (2)°, and γ = 92.48 (2)°. Least-squares refinement of the structure led to a final R factor (F basis) of 0.039 (R_w = 0.040) using 2384 independent reflections. The structure consists of stacks of centrosymmetrically related, nearly planar Cu(salphen) molecules, running in the c direction parallel to stacks of TCNQ molecules, whose spacing is twice that of the Cu(salphen) units. The geometry of the TCNQ molecule suggests the degree of charge transfer to be quite weak. Magnetic measurements from 9 to 295 K and the 77 K ESR spectrum show that there is no strong coupling between Cu(II) ions. The electrical conductivity, measured on a pressed powder at room temperature, $\sigma = 10^{-8}\ \Omega^{-1}\ cm^{-1}$, is 10 to 100 times higher than that of the starting materials. The overlapping of molecules of Cu(salphen) with molecules of TCNQ in the solid state is discussed.

Introduction

Molecular "charge transfer" or donor–acceptor adducts between various organic electron donors and acceptors have been known for many years and widely studied.[1-3] On the other hand, there are much fewer examples of charge-transfer complexes that are composed of transition-metal complexes and organic acceptors[4-10] or donors.[11-15] Both the strictly organic (i.e., the tetrathiafulvalene–tetracyanoquinodimethane-like compounds[16]) and the transition-metal complex

(1) Briegleb, G. "Zwischenmolekularkräfte"; G. Brown: Karlsruhe, 1949.
(2) Mulliken, R. S.; Person, W. B. "Molecular Complexes-A Lecture and Reprint Volume"; Wiley: New York, 1969.
(3) Herbstein, F. H. *Prespect. Struct. Chem.* **1971**, *4*, 166.
(4) Melby, L. R.; Harder, R. J.; Hertler, W. R.; Mahler, W.; Benson, R. E.; Mochel, W. E. *J. Am. Chem. Soc.* **1962**, *84*, 3374.
(5) Bailey, A. S.; Williams, R. J. P.; Wright, J. D. *J. Chem. Soc.* **1965**, 2579.
(6) Burgess, J.; Davis, K. M. C.; Kemmitt, R. D. W.; Raynor, J. B.; Stocks, J. *Inorg. Chim. Acta* **1970**, *4*, 129.
(7) Castellano, E. E.; Hodder, O. J. R.; Prout, C. K.; Sadler, P. J. *J. Chem. Soc. A* **1971**, 2620.
(8) Masai, H.; Sonogashira, K.; Hagihara, N. *J. Organomet. Chem.* **1972**, *34*, 397.
(9) Keller, H. J.; Leichert, I.; Megnamisi-Belombe, M.; Nöthe, D.; Weiss, J. *Z. Anorg. Allg. Chem.* **1977**, *429*, 231.
(10) Mayerle, J. J. *Inorg. Chem.* **1977**, *16*, 916.
(11) Schmitt, R. D.; Wing, R. M.; Maki, A. *J. Am. Chem. Soc.* **1969**, *91*, 4394.
(12) Wudl, F.; Ho, C. H.; Nagel, A. *J. Chem. Soc., Chem. Commun.* **1973**, 923.
(13) Alcacer, L.; Maki, A. *J. Phys. Chem.* **1974**, *78*, 215.
(14) Interrante, L. V.; Browall, K. W.; Hart, H. R., Jr.; Jacobs, I. S.; Watkins, G. D.; Wee, S. H. *J. Am. Chem. Soc.* **1975**, *97*, 889.
(15) Interrante, L. V.; Bray, J. W.; Hart, H. R., Jr.; Kasper, J. S.; Piacente, P. A. *J. Am. Chem. Soc.* **1977**, *99*, 3523.

0020-1669/80/1319-0665$01.00/0